

THE 166.6 MHZ PROOF-OF-PRINCIPLE SRF CAVITY FOR HEPS-TF

P. Zhang*, J. Dai, X. Hao, T. Huang, Z. Li, H. Lin, Q. Ma, F. Meng, Z. Mi, W. Pan, Y. Sun, G. Wang, Q. Wang, X. Zhang, Institute of High Energy Physics (IHEP), Beijing, China

Abstract

The 166.6 MHz superconducting RF cavities have been proposed for the High Energy Photon Source (HEPS), a 6 GeV kilometer-scale light source. The cavity is of quarter-wave type made of bulk niobium with $\beta=1$. Each cavity will be operated at 4.2 K providing 1.2 MV accelerating voltage and 145 kW of power to the electron beam. During the HEPS-Test Facility (HEPS-TF) phase, a proof-of-principle cavity has been designed in IHEP and manufactured in Beijing. The subsequent BCP was conducted in Ningxia, while HPR, cleanroom assembly and 120 degree bake was done in IHEP. The cavity was finally vertical tested at both 4.2 K and 2 K in IHEP. The cavity Q_0 at designed gradient (when $V_c=1.5$ MV) at 4.2 K was measured to be 2.4×10^9 with E_{peak} of 42 MV/m and B_{peak} of 65 mT. The maximum E_{peak} and B_{peak} reached 86 MV/m and 131 mT respectively at both 4.2 K and 2 K, and the corresponding Q_0 was measured to be 5.1×10^8 (4.2 K) and 3.3×10^9 (2 K). The residual surface resistance was measured to be 2.3 n Ω .

INTRODUCTION

High Energy Photon Source (HEPS) is a 6 GeV storage ring light source with kilometer-scale circumference and ultra-low emittance [1]. It has been proposed by IHEP and is planned to be built in Beijing suburb. The electron beam is firstly accelerated to 300 MeV by a linac and subsequently injected into a ~ 400 m booster ring to further ramp its energy to 6 GeV prior to its final injection into the ~ 1300 m storage ring. Its main beam parameters are listed in Table 1. Prior to its official construction, a test facility namely HEPS-TF has been approved in 2016 to R&D and prototype key technologies and key components.

Table 1: Beam Parameters of the HEPS Storage Ring

Parameter	Value
Energy	6 GeV
Circumference	~ 1300 m
Current	200 mA
Energy loss w/ IDs	2.5 MeV/turn
Total SR power	500 kW

A double-frequency RF system has been conceived to realize the recently proposed on-axis injection scheme [2]. The fundamental RF frequency has been chosen to be 166.6 MHz while the third harmonic RF is 499.8 MHz [3]. This scheme will make two stable RF buckets to enable the merging of the injected bunch into the circulating beam. The high harmonic RF system needs to be active rather than passive.

* zhangpei@ihep.ac.cn

The choice of the fundamental RF frequency is made by compromising competing demands of the kicker and the RF system. The state-of-art kicker has a total width of a few nano-seconds and favors a larger separation of the RF buckets, in other words, a lower RF frequency. On the other hand, a higher frequency will make the RF system more compact. Furthermore, in order to use as much as possible the mature technology of 500 MHz superconducting cavities, the main RF frequency has thus been chosen to be 166.6 MHz, one third of 499.8 MHz. Therefore the 166.6 MHz RF system naturally becomes the focus of the R&D during HEPS-TF phase.

Given the relatively low RF frequency (166.6 MHz), both normal conducting (NC) and superconducting (SC) options have been considered. A detailed comparison of these two options are given in [3]. This paper will focus on the 166.6 MHz SC cavity, in particular, the newly designed proof-of-principle cavity.

THE RF DESIGN

The Proof-of-Principle (PoP) cavity has been planned as the first cavity to be built in order to maximize learning on cavity manufacturing techniques, surface treatment and higher order mode (HOM) characterization. The cavity shall capture as many as possible the features which will be used in the final cavity design to ensure the experiences obtained are most relevant.

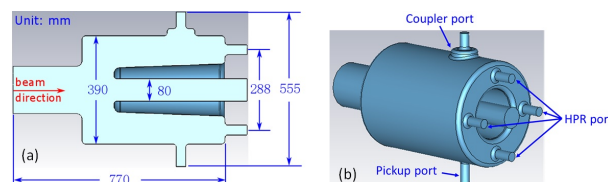


Figure 1: The 166.6 MHz PoP cavity.

Due to a low RF frequency and $\beta=1$, the popular elliptical shape will make the cavity geometry excessively large ($\beta \cdot \lambda/2$) thus unpractical for manufacturing. The quarter-wave cavity has then been chosen. The RF design and optimization were conducted within the following boundaries: firstly, the outer conductor radius is preferably to be less than 250 mm while keeping the inner conductor as big as possible, this is to ensure a manageable cavity size, larger beam aperture and larger helium volume inside the inner conductor; secondly, the peak electric field (E_{peak}) and peak magnetic field (B_{peak}) at design gradient ($V_c=1.5$ MV) needs to be less than ~ 40 MV/m and ~ 65 mT respectively, and this reserves 20% margin in peak fields when operating at nominal gradient ($V_c=1.2$ MV); thirdly, the frequency of the first dipole mode needs to be higher than 400 MHz to ensure

a larger frequency separation from the fundamental mode and consequently enables an effective HOM damping. A preliminary study on HOM damping scheme can be found in [4].

Table 2: The main RF Parameters of the PoP Cavity

Parameter	Value	
Operating temperature [K]	4.2	
V_c [MV]	1.5	
E_{acc} [MV/m]	14.5	
Q_0 at $V_c=1.5$ MV	$>1 \times 10^9$	
Parameter	CST	HFSS
R/Q ($=V_c^2/P$) [Ω]	136	136
G ($=R_s \cdot Q_0$) [Ω]	54	55
E_{peak} at $V_c=1.5$ MV [MV/m]	42	40
B_{peak} at $V_c=1.5$ MV [mT]	64	66
Stored energy [J]	15.8	15.8

The optimized cavity geometry is shown in Fig. 1 and its main RF parameters are listed in Table 2. The inner conductor is tapered in order to improve the liquid helium flow and lower the risk of gas trapping. The electromagnetic field distribution of the fundamental mode is shown in Fig. 2 and Fig. 3 is the accelerating field profile on the beam axis. The results from two simulation codes are consistent. Both codes are converged to a relative frequency error below $3e-5$ corresponding to ~ 4 kHz.

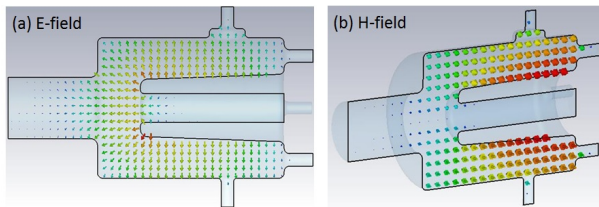


Figure 2: The electromagnetic field of the PoP cavity.

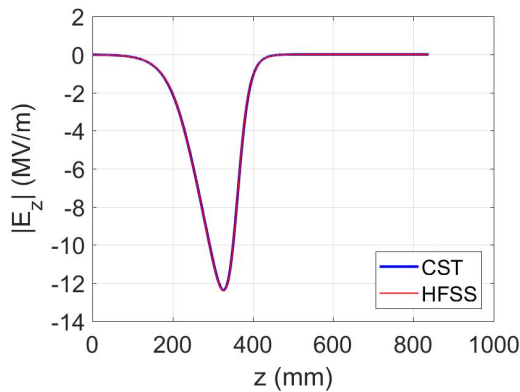


Figure 3: The electric field on beam axis simulated by using CST MWS [5] and ANSYS Electromagnetic Suite [6].

The cavity has multiple ports opened on its outer conductor for different purposes as defined in Fig. 1(b). A minimum

number of 4 HPR (High Pressure Rinsing) ports are required to ensure a proper coverage of rinsing water on the inner conductor surface as shown in Fig. 4. On the other hand, HPR ports are located in the high magnetic field region, more ports will increase the risk of contamination thus lower the cavity Q_0 . In addition, cares must be taken to prevent field enhancement by adding these ports on the cavity end plate. The dependence of the peak magnetic field on the blending radius of the HPR ports connecting to the plate is shown in Fig. 5. Once the blending radius is larger than 10 mm, B_{peak} fulfills our previously mentioned requirement, and a blending radius of 11 mm was finally chosen.

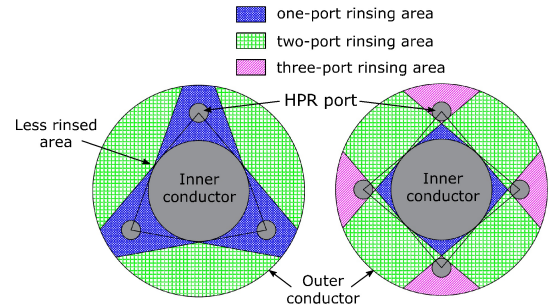


Figure 4: The choice of HPR ports.

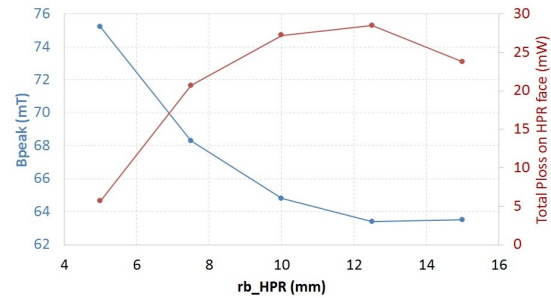


Figure 5: The dependence of B_{peak} and port surface loss on the blending radius of the HPR port.

During cavity vertical test at 4.2 K, all ports will be closed with stainless steel blind flanges. In order to ensure a minimum RF heating on these normal conducting flanges, the length of each port has been optimized. In addition, a short piece of cut-off tube is added to the coupler port to lower the RF leakage and consequently reduce the cavity transverse size. The results of the RF heating at designed field level adds up to 37 mW additional loss to the cavity corresponding to a Q value of

$$Q_{flange} = \frac{\omega U}{P_{loss}} = \frac{2\pi \cdot 166.6e6 \cdot 15.8}{0.037} = 4.5 \times 10^{11}. \quad (1)$$

This is negligible comparing to the cavity Q_0 of $\sim 10^9$.

THE MECHANICAL DESIGN AND CAVITY FABRICATION

The mechanical design of the PoP cavity was conducted in-house. The model of the bare cavity is shown in Fig. 6.

Content from this work may be used under the terms of the CC BY 3.0 licence (© 2017). Any distribution of this work must maintain attribution to the author(s), title of the work, publisher, and DOI.

The wall thickness varies from 3.5 mm to 5 mm for different components. The mechanical properties of the cavity were studied by using ANSYS® simulation suite. The results of cavity rigidity, frequency sensitivity to helium pressure variation, Lorentz force detuning and microphonics are presented in detail in [7].

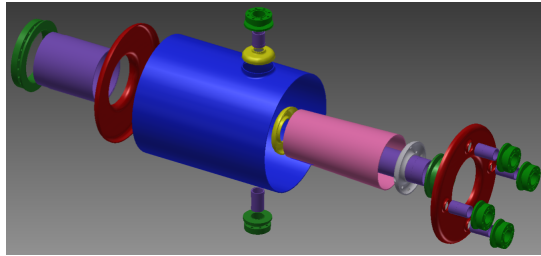


Figure 6: The PoP cavity components.

The cavity was then contracted to *Beijing HE-Racing Technology Co., Ltd.* [8]. Some of the key fabrication processes and components are shown in Fig. 7. Deep drawing and electron-beam welding were used during the production. The fabrication details are described in [7].

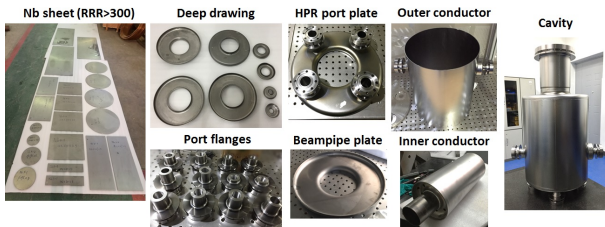


Figure 7: The fabrication of the PoP cavity.

THE CAVITY TREATMENT AFTER FABRICATION

After fabrication, the cavity was sent to Ningxia for surface treatment. Every welding was grinded using 40 μm sandpaper before BCP for initial smoothing. A 75' BCP was conducted first with the HPR plate facing upwards as shown in Fig. 8. It's then followed by another 75' BCP by making the cavity upside down to obtain a uniform etching. Consequently 160 μm was removed on the two end plates while 110 μm on the outer conductor and beam pipe. The etching speed and uniformity were controlled by cooling the cavity from outside using tap water during BCP. The thickness of the cavity outer wall was measured by ultrasonic at selected locations after each etching. The cavity surface was then visually inspected and light polished by 16 μm sandpaper to achieve an even smoother surface. The cavity was subsequently annealed at 750°C for 3 hours in a vacuum furnace. Finally a 30' light BCP was conducted to wrap the etching campaign.

The cavity was then sent back to IHEP in Beijing for HPR, cleanroom assembly and 120°C bake followed by a frequency pre-tuning [9]. At this point, the cavity is ready

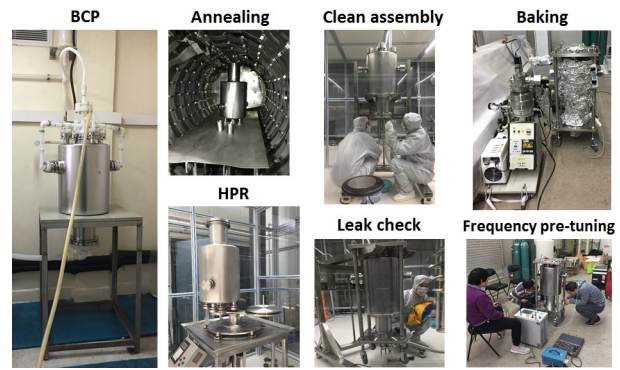


Figure 8: The treatment of the PoP cavity.

for vertical test. Table 3 lists all the treatment processes and more details can be referred to [10].

Table 3: The Cavity Treatment Processes

No.	Process
1	75' BCP (HPR plate facing upwards)
2	75' BCP (HPR plate facing downwards)
3	3-hour annealing at 750°C
4	30' light BCP (HPR plate facing upwards)
5	HPR (from 6 ports, 60' each)
6	Clean assembly in Class 100 cleanroom
7	48-hour baking at 120°C
8	Frequency pre-tuning

THE VERTICAL TEST

The cavity was installed on a supporting frame where four titanium rods were used to stiffen the cavity as shown in Fig. 9. This prevents the cavity from plastic deformation when pumping to vacuum and cooling down to cryogenic temperatures. The cryogenic vertical test was conducted in IHEP at both 4.2 K and at 2 K. A mobile coupler was used to maintain a critical coupling during the measurements. The Q_0 vs. E_{acc} curves were measured and shown in Fig. 9. The cavity Q_0 at designed gradient (when $V_c=1.5$ MV) at 4.2 K was measured to be 2.4×10^9 with E_{peak} of 42 MV/m and B_{peak} of 65 mT. The maximum E_{peak} and B_{peak} reached 86 MV/m and 131 mT respectively at both 4.2 K and 2 K. The corresponding Q_0 at highest field was measured to be 5.1×10^8 (4.2 K) and 3.3×10^9 (2 K). The measured results largely exceed the design goal. The onset of field emission starts at $E_{acc} \sim 17$ MV/m for 4.2 K and $E_{acc} \sim 15$ MV/m for 2 K, then steadily went up by five order of magnitude before quenching at the highest field as shown in Fig. 10.

The dependence of surface resistance on the cavity temperature was measured during pumping from 4.2 K to 2 K and is shown in Fig. 11(a). The fitted residual resistance was 2.3 n Ω , proving a successful cavity treatment.

The temperature of the cavity was monitored by two Cernox sensors mounted on the top and bottom of the cavity outer wall. Fig. 11(b) shows the temperature readouts of the

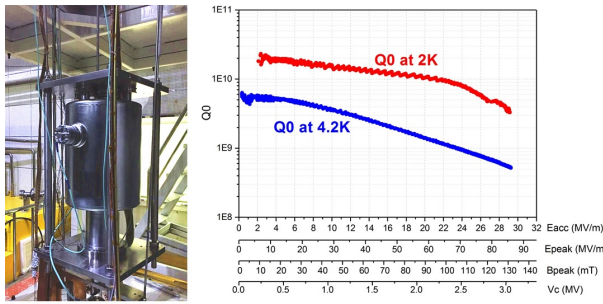


Figure 9: The cavity on the vertical test stand and the measured Q_0 vs. E_{acc} curve.

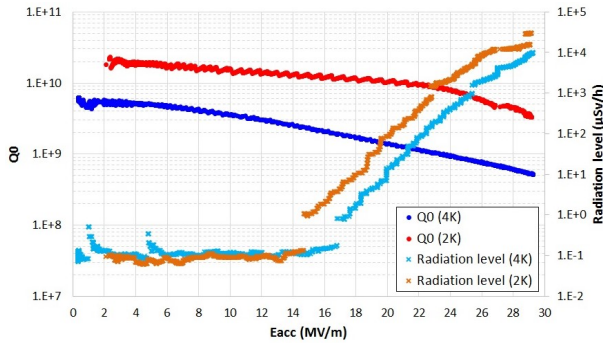


Figure 10: The Q_0 vs. E_{acc} curve along with radiation level.

cooldown process from room temperature to 4.2 K. The cavity was parked at 15 K for about 2 hours before going down to 4.2 K due to technical reasons of the cryogenics system. This however gives the cavity sufficient time to thermalize and consequently results in a rather small temperature gradient (2.4 K) but slow transition from SC to NC (5 mK/s). The cavity was shielded from the Earth’s magnetic field during the cold test and the residual ambient field at the cavity position was measured to be $\sim 1\mu\text{T}$ at room temperature. This will amount to 1.2 n Ω in the measured residual resistance [11]. Given the rather homogeneous cooldown and low ambient magnetic field, an optimized residual resistance might have been achieved in terms of flux trapping [12]. The cooldown dynamics is summarized in Table 4.

Table 4: The Cooldown Condition

Parameter	Value
Cavity top	11.6 K
Cavity bottom	9.2 K
ΔT through T_c	2.4 K
Δt through T_c	7.6 min
Transition rate	5 mK/s

FINAL REMARKS

A 166.6 MHz superconducting RF system has been proposed for HEPS project. A proof-of-principle 166.6 MHz SRF cavity has been designed, fabricated, post-processed and cryogenic tested. The results largely exceed the design

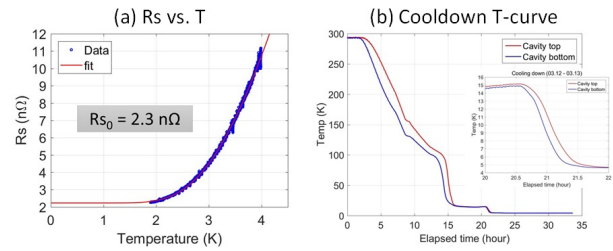


Figure 11: The surface resistance vs. temperature and the temperature readout during cooldown.

goal. This serves as a good starting point to proceed with the final cavity design where higher order mode damping is a key issue and is currently under intensive study.

ACKNOWLEDGEMENTS

We thank Q. Qin for his encouragement and constant support. We are grateful to R. Ge and Z. Fan for their technical support. We also appreciate R. Rimmer, G. Burt, T. Furuya, J. Liu, K. Liu, O. Napoly, Q. Wu and Z. Zhao for enlightening discussions. This work has been supported by HEPS-TF project and partly by Pioneer “Hundred Talents Program” of Chinese Academy of Sciences.

REFERENCES

- [1] Y. Jiao *et al.*, “Progress of the Physical Design and Studies on the High Energy Photon Source,” in *Proceedings of IPAC2017*, pp. 2697–2699, 2017.
- [2] G. Xu *et al.*, “On-axis Beam Accumulation Enabled by Phase Adjustment of a Double-frequency RF System for Diffraction-limited Storage Rings,” in *Proceedings of IPAC2016*, pp. 2032–2035, 2016.
- [3] P. Zhang *et al.*, “A 166.6 MHz Superconducting RF System for the HEPS Storage Ring,” in *Proceedings of IPAC2017*, pp. 1049–1051, 2017.
- [4] X. Hao *et al.*, “Hom Damping With an Enlarged Beam Tube for Heps 166.6 MHz SC Cavities,” in *these proceedings*, 2017. TUPB004.
- [5] CST Microwave Studio®. Ver. 2017, CST AG, Germany.
- [6] ANSYS® Electromagnetics Suite. Ver. 18, ANSYS, Inc., USA.
- [7] X. Zhang *et al.*, “The 166.6 MHz Proof-of-Principle SRF Cavity for HEPS-TF: Mechanical Design and Fabrication,” in *these proceedings*, 2017. TUPB037.
- [8] <http://www.he-racing.com/>.
- [9] P. Zhang *et al.*, “Frequency Pre-tuning of the 166.6 MHz Proof-of-Principle SRF Cavity for HEPS-TF,” in *these proceedings*, 2017. TUPB035.
- [10] J. Dai, “Post Processing of a 166MHz HEPS-TF Cavity at Institute of High Energy Physics (IHEP),” in *these proceedings*, 2017. TUPB083.
- [11] H. Padamsee *et al.*, *RF Superconductivity for Accelerators*, ch. 9.3, p. 174. Wiley-VCH, 2 ed., 2008.

- [12] J.-M. Vogt *et al.*, “Impact of cool-down conditions at T_c on the superconducting rf cavity quality factor,” *Phys. Rev. ST Accel. Beams*, vol. 16, 2013.